
Electronic Theses and Dissertations, 2004-2019

2019

Variable Fluid Flow Regimes Alter Endothelial Adherens Junctions and Tight Junctions

Dilshan Ranadewa
University of Central Florida

 Part of the [Mechanical Engineering Commons](#)
Find similar works at: <https://stars.library.ucf.edu/etd>
University of Central Florida Libraries <http://library.ucf.edu>

This Masters Thesis (Open Access) is brought to you for free and open access by STARS. It has been accepted for inclusion in Electronic Theses and Dissertations, 2004-2019 by an authorized administrator of STARS. For more information, please contact STARS@ucf.edu.

STARS Citation

Ranadewa, Dilshan, "Variable Fluid Flow Regimes Alter Endothelial Adherens Junctions and Tight Junctions" (2019). *Electronic Theses and Dissertations, 2004-2019*. 6339.
<https://stars.library.ucf.edu/etd/6339>

VARIABLE FLUID FLOW REGIMES ALTER ENDOTHELIAL ADHERENS
JUNCTIONS AND TIGHT JUNCTIONS

by

DILSHAN RANADEWA
B.S. University of Central Florida, 2016

A thesis submitted in partial fulfillment of the requirements
for the degree of Master of Science
in the Department of Mechanical and Aerospace Engineering
in the College of Engineering and Computer Sciences
at the University of Central Florida
Orlando, Florida

Spring Term
2019

Major Professor:
Robert Steward Jr.

©2019 by Dilshan Ranadewa

ABSTRACT

Variable blood flow regimes influence a range of cellular properties ranging from cell orientation, shape, and permeability: all of which are dependent on endothelial cell-cell junctions. In fact, cell-cell junctions have shown to be an integral part of vascular homeostasis through the endothelium by allowing intercellular signaling and passage control through tight junctions (TJs), adherens junctions (AJs), and gap junctions (GJs). It was our objective to determine the structural response of both AJs and TJs under steady and oscillatory flow. Human brain microvascular endothelial cells (HBMECs) were cultured in a parallel plate flow chamber and exposed to separate trails of steady and oscillatory fluid shear stress for 24 hours. Steady flow regimes consisted of a low laminar flow (LLF) of 1 dyne/cm², and a high laminar flow (HLF) of 10 dyne/cm² and oscillatory flow regimes consisted of low oscillatory flow (LOF) +/- 1 dyne/cm² and high oscillatory flow (HLF) of +/- 10 dyne/cm². We then imaged the TJs ZO-1 Claudin-5 and AJs JAM-A VE-Cadherin and subsequently analyzed their structural response as a function of pixel intensity. Our findings revealed an increase in pixel intensity between LLF and LOF along the boundary of the cells in both TJs ZO1 Claudin 5. Therefore, our results demonstrate the variable response of different cell-cell junctions under fluid shear, and for the first time, observes the difference in cell-cell junctional structure amongst steady and oscillatory flow regimes.

TABLE OF CONTENTS

LIST OF FIGURES	v
LIST OF TABLES	vi
INTRODUCTION	1
CHAPTER 1 METHODOLOGY	7
1.1 Cell Culture and Preparation	7
1.2 Chamber Preparation	7
1.3 Experimental Setup.....	8
1.4 Fluid Shear Experiment.....	9
1.5 Immunohistochemistry	10
CHAPTER 2 POST PROCESSING	12
2.1 Data Acquisition/Imaging	12
2.2 Method of Analysis	13
CHAPTER 3 RESULTS.....	14
3.1 ZO-1 Measured Length Data	14
3.2 Claudin-5 Measured Length Data.....	15
3.3 JAM-A Measured Length Data	16
3.4 VE-Cadherin	17
3.5 Results Comparison	18
CHAPTER 4 DISCUSSION	20
LIST OF REFERENCES.....	22

LIST OF FIGURES

Figure 1: 0.4 Luer Ibbidi Laminar Flow Chamber.....	8
Figure 2: Experimental Setup.....	9
Figure 3: Images from Immunohistochemistry.....	11
Figure 4: Protein Intensity Measurement.....	12
Figure 5: Sample ImageJ Measurement Output.....	13
Figure 6: Graph of ZO-1 Protein Intensity	14
Figure 7: Graph of Claudin-5 Protein Intensity	15
Figure 8: Graph of JAM-A Protein Intensity	16
Figure 9: Graph of VE-Cadherin Protein Intensity	17
Figure 10: Average Protein Comparison Graph	18

LIST OF TABLES

Table 1: Table of Average Protein Intensity Comparison.....	19
Table 2: Paired Student t-Test Results.....	19

INTRODUCTION

Throughout the body's vasculature, we find a constant blood flow that meets a thin sheet of cells which lines the innermost walls. Endothelial cells. Endothelial cells (ECs) have multiple functions however some of the most noted are their ability to regulate the passage of material between the bloodstream and the tissue, their role in blood flow regulation and importantly, they are vital to vascular homeostasis. We find this endothelium throughout the body's vasculature however ECs organization differs depending on the location of the vasculature. In areas where blood solute permeability is less regulated we find that the ECs are less tightly compact allowing for easier passage of materials from the bloodstream through to the rest of the body. However, in areas of vasculature where solute permeability needs to be highly regulated such as the brain, we find EC organization is extremely compact and tightly bonded together to restrict passage through the endothelium. This type of vasculature found in the brain is termed the blood brain barrier (bbb). It is one of the most unique areas of vasculature found in the body due to its semipermeable barrier ability that is the most highly regulated areas in our body.

The bbb is slightly different from other pieces of vasculature because it's constructed with neuronal cells --astrocytes and pericytes--which surround the endothelium. Astrocytes work as a scaffolding cell whose feet form around the pericytes and ECs to hold the structure of the vasculature together; pericytes are found around the brain endothelium and help with vasoconstriction and dilation (Taddei). This formation of cells works together to create the bbb which is essential supplying the brain nutrients and to mediate the efflux of the waste products from the central nervous system back into the bloodstream.

ECs functionality stems from the different types of junctional structures that allow communication, adhesion, and transport through the layer of endothelial cells. The layer of ECs are also called the endothelium is found throughout our body's vasculature and are connected together by transmembrane junctional proteins. These junctional structures are made up transmembrane adhesion proteins. In epithelial cells there are four specific types; adherens junctions (AJs), tight junctions (TJs), gap junctions (GJs) and desmosomes.

These proteins are responsible for endothelial cell-cell adhesion, communication, and controls permeability through the cell monolayer. AJ's role in the endothelium are closely linked to intercellular adhesion which is seen in AJ specific proteins called cadherins, these proteins attach scaffolding proteins called catenins which in turn attach to actin filaments found on the cytoskeleton of the cell. They connect endothelial cells together by gripping to adjacent cadherin proteins which are supported by this transmembrane interaction. AJs such as VE-cadherin are found throughout the body's endothelium and are generally found closer to the basal membrane of the endothelium. These junctional proteins have been directly linked to supporting the functions of TJs (Miao). TJs, also responsible for cell-cell adhesion, the junctional protein responsible for the regulation of solutes through endothelium. They are apical junctions found closer to the top of the endothelium which assist their roll on regulating what goes through the ECs. The combination of TJs and AJs and the amount present differs in various parts of the endothelium found in the body. Due to the highly restrictive nature of the bbb, the presence of junctional proteins is much larger in the brain than the rest of the body's vasculature, specifically with respect to TJs. Major types of TJs found in the bbb endothelium include claudins, occludins, and JAM proteins.

The imbalance of ions and metabolic products from the bloodstream through the vasculature is hallmark of vascular dysfunction. This influx of excess material is extremely detrimental in brain due to the sensitive neuro environment of the central nervous system. Studies have shown that bbb dysfunction, has been linked to the regulation of junctional proteins which have been directly linked to almost all neurodegenerative diseases. Diseases such as Multiple sclerosis has a direct impact on TJ presence in brain, case studies have shown a downregulation in TJs in patients which lead to an increase on solute permeability (Cucullo). This increase in solute permeability disrupts brain homeostasis, further preventing efflux of waste out of the CNS. The dysfunction of the bbb can be influenced by certain general vascular diseases as well.

Atherosclerosis is one of the deadliest vascular diseases that affects millions of people each year and impacts vasculature throughout the body. This vascular disease is responsible for the hardenings of the veins and the formation of atherosclerotic plaque build which is detrimental to vascular homeostasis. In cerebral atherosclerosis, hardening of the vasculature and plaque buildup have been shown to impact vascular regulation through the bbb and due to the small cross-sectional area of vasculature found in the brain, plaque build ups specifically has been directly linked to early stages of stroke. Studies have shown that cerebral pathologies are also linked to the influence of the hemodynamic force exerted by the constant blood flow throughout the body.

Influence of fluid shear

ECs exist in one of the most mechanically enriched environments in the body. There exists a constant cyclical strain and fluid shear stress exerted on the ECs which in turn generate intracellular stresses that act upon the vasculature. When one considers the hemodynamic forces the pressure exerted by heart pumping is also influential in vascular homeostasis. However pressure due to heart pumping is dampened as blood flows throughout the vasculature. Studies have shown that pressure is significantly damped in the brain to the extent that which cyclical strain due to pressure can almost be neglected. Thus, when analyzing the forces due to blood in the brain, scientist focus on the fluid shear stress in the vasculature. Understanding how fluid shear influences EC functionality begins with understanding the different flow regimes found in the brain. The characterization of fluid flow patterns is determined using the Reynolds number. These flow regimes can be characterized as laminar which has a Reynolds number less than 2300, turbulent which has a Reynolds number of more than 4000 and transitional which has a Reynolds number between 2300 and 4000. Aside from traditional fluid flow patterns, disturbed and pscillatory flows can also be found within the brain; disturbed flow being defined as change in a laminar flow pattern caused by a change in geometry and oscillatory flow happens when fluid flow oscillates back and forth with no net mean change in direction of flow. Scientist have shown that the Reynolds number found in the brain is around 100 making the flow in the brain generally laminar flow.

Changes in blood flow patterns are generally caused by geometric changes in the body's vasculature which are found in areas of bifurcation, change in direction, and in areas with atherosclerotic plaque buildup. This change in fluid flow patterns has a direct impact on the magnitude of fluid shear exerted on the endothelium. It has been noted that typical fluid shear stress found in the bbb ranges from 1-10 dyne/cm² (Colgan).

When studying fluid shear stress on the brain endothelium in-vitro, researchers use various type of chambers to mimic the neuronal environment found within the brain. These fluid flow chambers contain a microchannel in which where cells are cultured and exposed to conditions closely related to their naturally-occurring physiological area. When calculating the fluid shear stress along the endothelium in vitro, researchers establish boundary conditions which call for certain assumptions to be made. Calculation of fluid shear stress in a rectangular microchannel calls for the assumptions that the fluid is incompressible and steady. These assumptions are used when the fluid boundary layer is laminar and there exists a constant freestream of fluid. Even though this might not be the case throughout the body, due to the significant dampening of pressure from the heart to the brain, these assumptions can closely relate the physiological forces to an in vitro study. Ergo, when observing the system in 2D the derivation of the fluid shear stress begins from taking the governing equations which are reduced from Navier-Stokes equations. After mathematical manipulation using the governing equations and characteristics of the fluid flow, the equation of fluid shear can be extracted from the 2nd order differential equation in the form:

$$\tau_w = \frac{6\mu Q}{bh^2}$$

The equation for fluid shear stress along the wall, τ_w , is a formulation of the product of dynamic viscosity μ with the volumetric flowrate Q divided by the product of the length of the base b and the height h of the chamber (Noria).

We know that in the vasculature of the brain HBMECs that are induced to a fluid shear stress have shown to decrease molecular permeability. This change of permeability is assisted by the intercellular junctions of the endothelial cells. The intercellular junctions control communication and cell-cell adhesion which are connected through different signaling pathways (Stamatovic). Changes in junctional organization may affect cell-cell adhesion and communication which will have an overall effect on the vascular homeostasis of the brain. Cell-Cell junctions have shown to be an integral part of vascular regulation through the endothelium by allowing intercellular signaling and passage control through TJs and AJs (Sei). Studies have shown certain pathologies of the brain affect cell-cell junctions drastically which leads to major bbb disruption. Junctional complex remodeling is associated with different neurocognitive diseases such as certain cancers, autoimmune disorders, and more commonly cerebral atherosclerosis. Atherosclerotic plaque forms in bifurcated regions in the brain and has been found experimentally in regions with lower fluid shear stress and oscillatory flow; by manipulating these conditions, the junctional response can be studied.

CHAPTER 1 METHODOLOGY

1.1 Cell Culture and Preparation

An immortalized HBMEC cell-line at passage 25 were purchased from Fisher Scientific, and grown in T75 flasks with EndoGro Basal cell medium. The cells were stored in an incubator at 37°C with 5% CO₂. Once flasks became confluent (48 hours) cells were detached using trypsin 0.5 1X for 4 minutes then placed in a centrifuge for 3 minutes at 3000 RPM. The cells are then re-suspended in 1mL of HBMEC Basal media (average density of 5.00×10^6 cell/mL media) and 300 uL of that re-suspended cell solutions is used to fill the Ibidi 0.4 Luer Flow Chamber. The remaining suspension is passaged into a t75 for further experiments. HBMECs were left in the Ibidi flow chamber for 24 hours until fully confluent, then chambers were attached to a flow specific flow loop and respective experiments were conducted.

1.2 Chamber Preparation

Ibidi 0.4 Luer single plate flow chambers were ordered from the distributor. Chamber assembly began with detaching the adhesive paper from the chamber and combining a microscope glass slide to the opened adhesive side. Once chambers were constructed, a silicon epoxy was added around the perimeter of the chamber to insure a tight leak proof seal; chambers were placed in the refrigerator for 24 hours for the epoxy to set. Following the sealing protocol, chambers were rinsed with PBS two times and a .15% Collagen 4 solution was added, chambers were set in the incubator for 1 hour (collagen polymerization) then taken out and rinsed with PBS.

1.3 Experimental Setup

Shear experiments were conducted in the incubator (37°C with 5% CO₂). The flow rate was controlled by a KDscientific peristaltic flow pump and each shear experiment was programmed with multiple step functions. The low shear experiment begins with 0 flow rate and gradually increases to 1.15723 mL/min over a 30-minute interval, the program then proceeds to run the end flow rate of 1.15734 mL/min for 24 hours. This step function is used for every flow regime to ensure cell attachment to the surface. Flow rates were calculated given dimensions from Ibidi 0.4 Luer which has the dimensions of 0.027 m, height of 0.006197m and a dynamic viscosity of water at 37°C of 0.6913 mPa.s. The constants were plugged into the equation of shear force along the wall and flow rates were calculated based off 1 and 10 Dynes/cm². Figure 1 is an image of the Ibidi 0.4 Luer laminar flow chambers used; the two cylindrical openings are the inlet and outlets used, which are attached to the flow loop.



Figure 1: 0.4 Luer Ibidi Laminar Flow Chamber

1.4 Fluid Shear Experiment

Laminar low- and high-shear experiments we conducted in a cell culture incubator at 37°C and 5% CO₂. Ibidi 0.4 Luer chambers were cultured with HBMEC until fully confluent. Once chambers were confluent, they were attached to the flow; the flow loops begins with 30 minute cycle of gradually increasing shear stress until desired low or high flow rate is met. After 30 minutes, the pump dispenses the final desired flow rate for 24 hours (LLF = 1 dyne/cm², HLF = 10dyne/cm²). Samples are taken out of the flow loop, fixed with formaldehyde, and stained for respective junctions. Oscillatory shear experiments we conducted in a cell culture incubator at 37°C and 5% CO₂. Ibidi 0.4 Luer chambers were cultured with HBMEC until fully confluent.

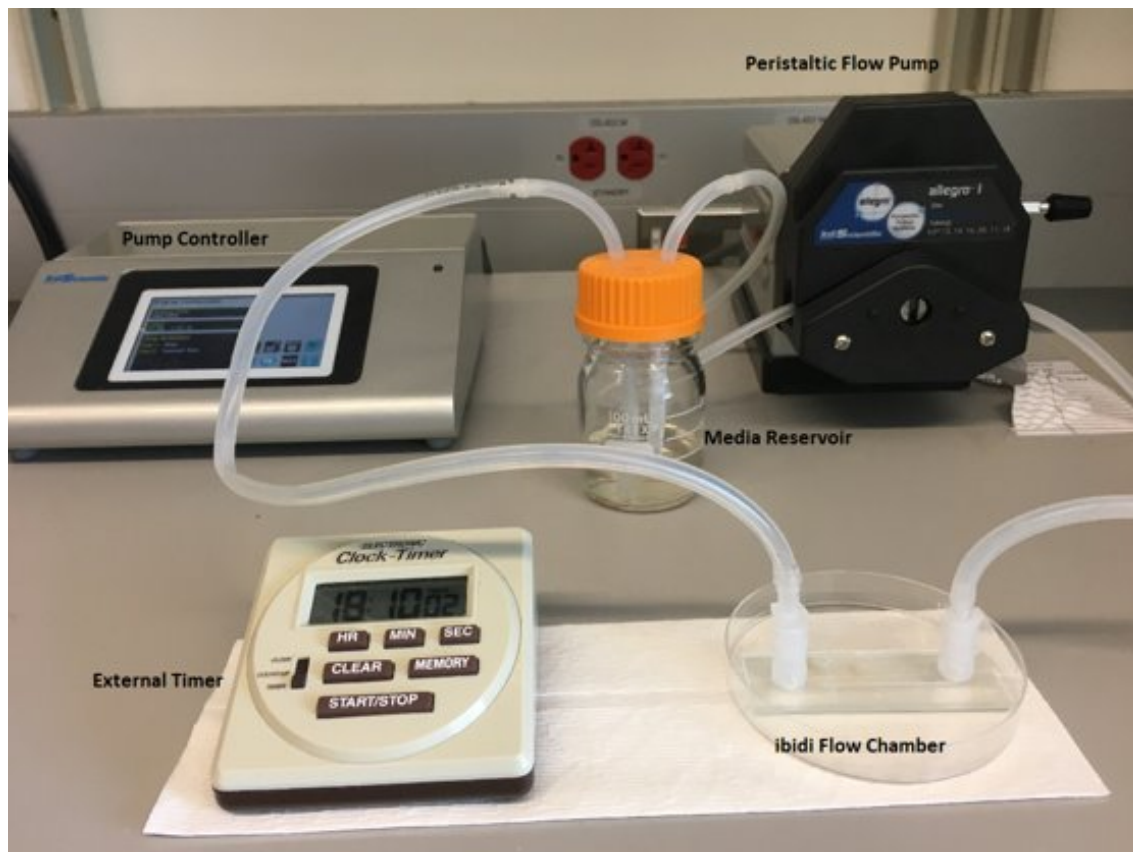


Figure 2: Experimental Setup

Once the chambers were confluent, they were attached to the flow; the flow loops begins with 30 minute cycle of gradually increasing shear stress until desired low or high flow rate is met. Once the desired flow rate is met, the pump begins to dispense the flow rate in one direction then switches directions with the same flow rate at a frequency of 1 Hz (LOF = +/- 1 dyne/cm², HOF = +/- 10dyne/cm²).

The experimental set is shown in Figure 2 and shows the entire flow system connected; the Ibidi flow chamber is outside of the incubator to depict the experimental setup however during live experiments the flow chamber would remain inside the incubator. The media reservoir and chamber were both secured in the incubator to maintain 37°C and 5% CO₂ environment.

1.5 Immunohistochemistry

Once the shear experiments were successfully conducted (24 hours), samples were taken out of the flow loop and fixed with 4% formaldehyde (2mL) for 15 minutes in the incubator. Immediately after the fixing step, samples were rinsed twice with PBS and 0.2% Triton100 (2mL) was added (5 minutes in the incubator). During the fixing and permeabilizing steps, the primary antibody's were prepared for immediate application once the samples were finished permeabilizing. 5 uL of the primary antibody's of two proteins were mixed with 1 mL of PBS; ZO-1 and VE-Cadherin were used together one sample following with JAM-A and Claudin-5 combination for the other samples.

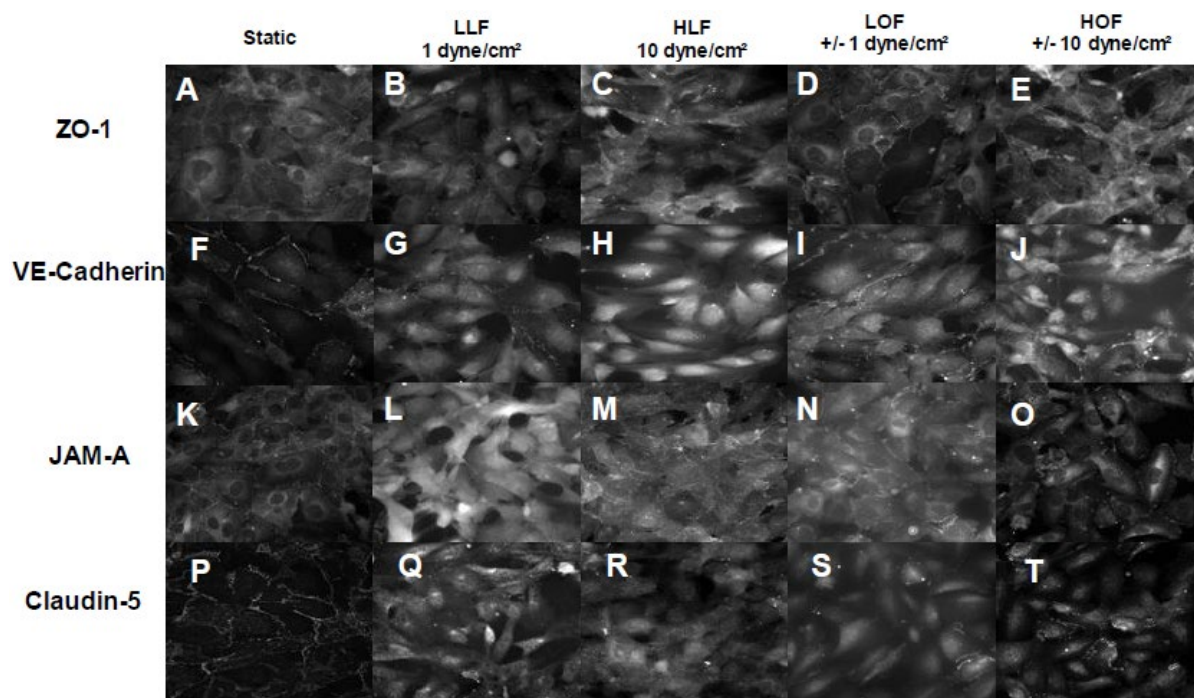


Figure 3: Images from Immunohistochemistry

After the Triton -X100 was rinsed twice with PBS we added a signal enhancer for 25 minutes then proceeded to add the primary antibody solution and the sample was placed in the refrigerator for 24 hours to set. After 24 hours, samples rinsed with PBS and treated with the secondary antibody that correlated with the respective primary antibody used on the sample. Following a 2 hour exposure to the secondary antibody, samples were with Fluoromount-G to keep them hydrated and a glass coverslip was then placed over the sample. The images shown in Figure 3 depicts a sample of each protein under the various flow regimes taken after the staining protocol had been completed. Imaging was conducted immediately after the samples were fixed with a glass cover slide.

CHAPTER 2 POST PROCESSING

2.1 Data Acquisition/Imaging

Images of the samples were taken using a Zeiss epifluorescence scanning microscope with a 63X oil emergent objective. Images were taken with a consistent position throughout each sample; exposure time were the same for all images taken. Images were analyzed using ImageJ image-processing software; images were uploaded to the software and a 350 pixel (56.9 micron) length line was drawn across the entirety of the cell. The average gray pixel intensity was measured along the length for 75 cells and the results were input to Microsoft Excel. Figure 4 is an example of how pixel intensity was measured across the cell.

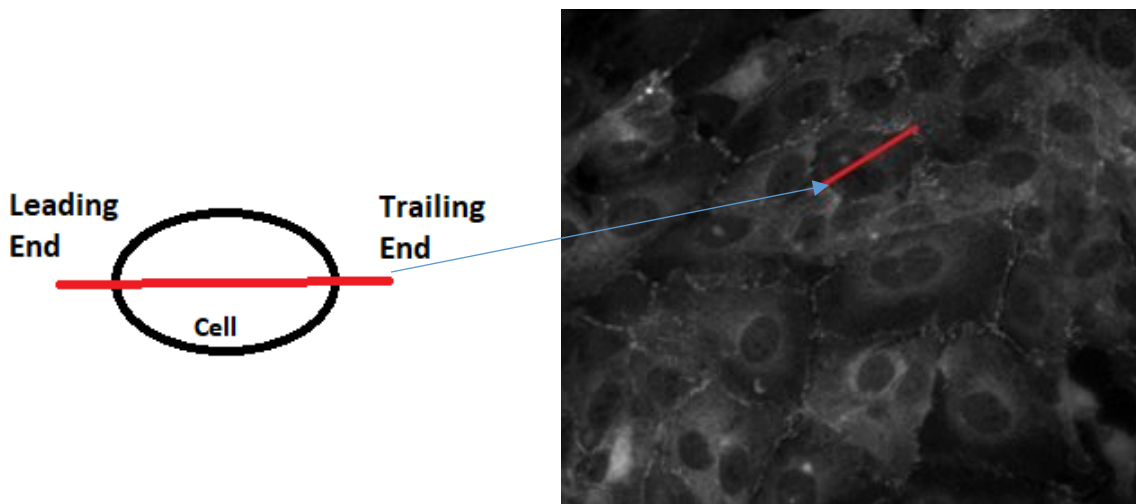


Figure 4: Protein Intensity Measurement

After the target cell was measured along the direction of flow, imageJ would output the mean gray value pixel intensity as shown in Figure 5. This process was done for 75 cells for each protein in all four flow regimes.

2.2 Method of Analysis

Once the measured pixel intensity data was taken from imageJ each measurement was input into excel for the respective protein. The results were then averaged over each pixel value from 1 to 350 and those average values were graphed. This graphed data depicts the average of 75 cells protein intensity along the measured length and allowed us to determine where the protein localized. The entire 350 pixel measurement length was then averaged to determine the overall mean gray value pixel intensity difference between each flow regime.

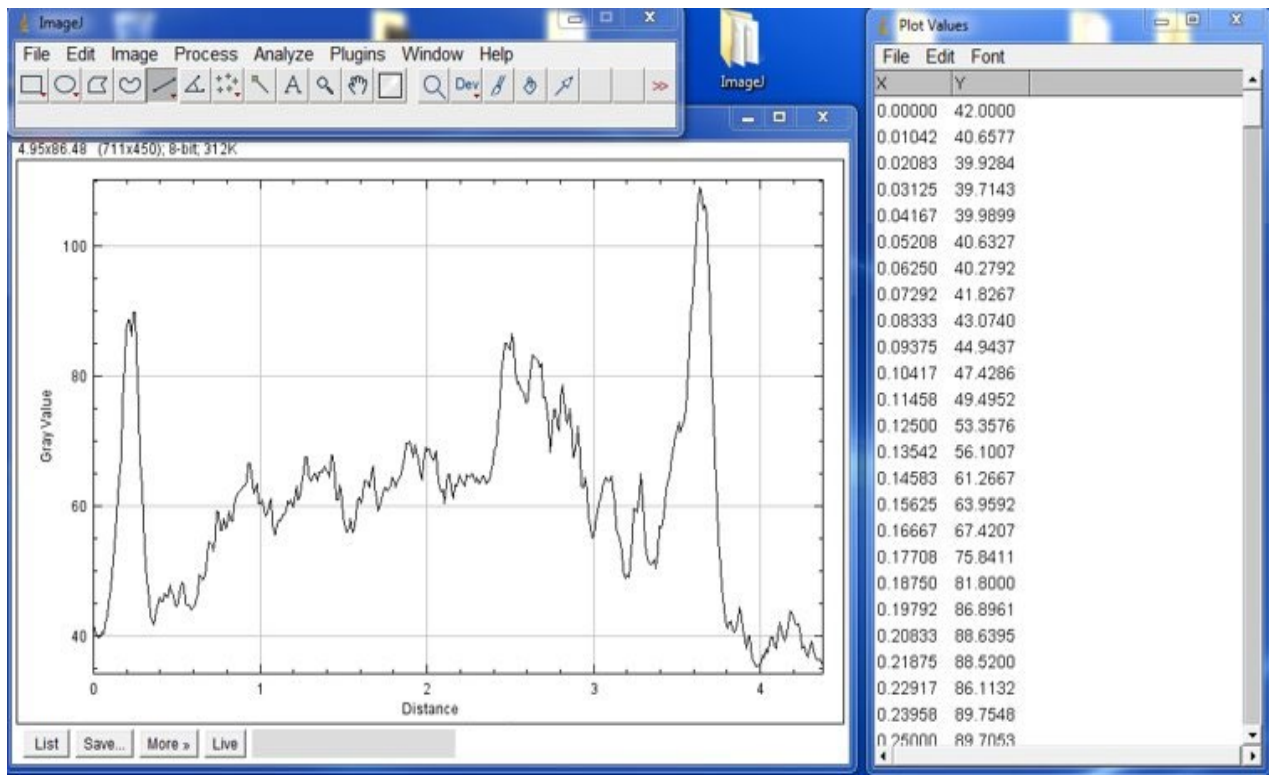


Figure 5: Sample ImageJ Measurement Output

CHAPTER 3 RESULTS

3.1 ZO-1 Measured Length Data

The results in the ZO-1 display a change in the junction intensity and structure that is clearly distinguishable between various flow regimes. The static images display a strong confluency and clear intensity around the periphery of the cell. The cell-cell junction structure of the LLF flow when compared the LOF shows an increase in pixel intensity around the periphery of the cell which can be seen in Figure 6. We see a consistent increase in pixel intensity on the LE and TE of the cell between LLF & LOF. All flow regimes show an increase in localization around the center of the measurements compared to the static condition. Pixel intensity decreases from LLF to HLF around the LE and TE of the measurements as well as the center of the measurement. There is also a decrease in periphery intensity from LOF to HOF; LLF displayed the highest localization around the center of the measurement.

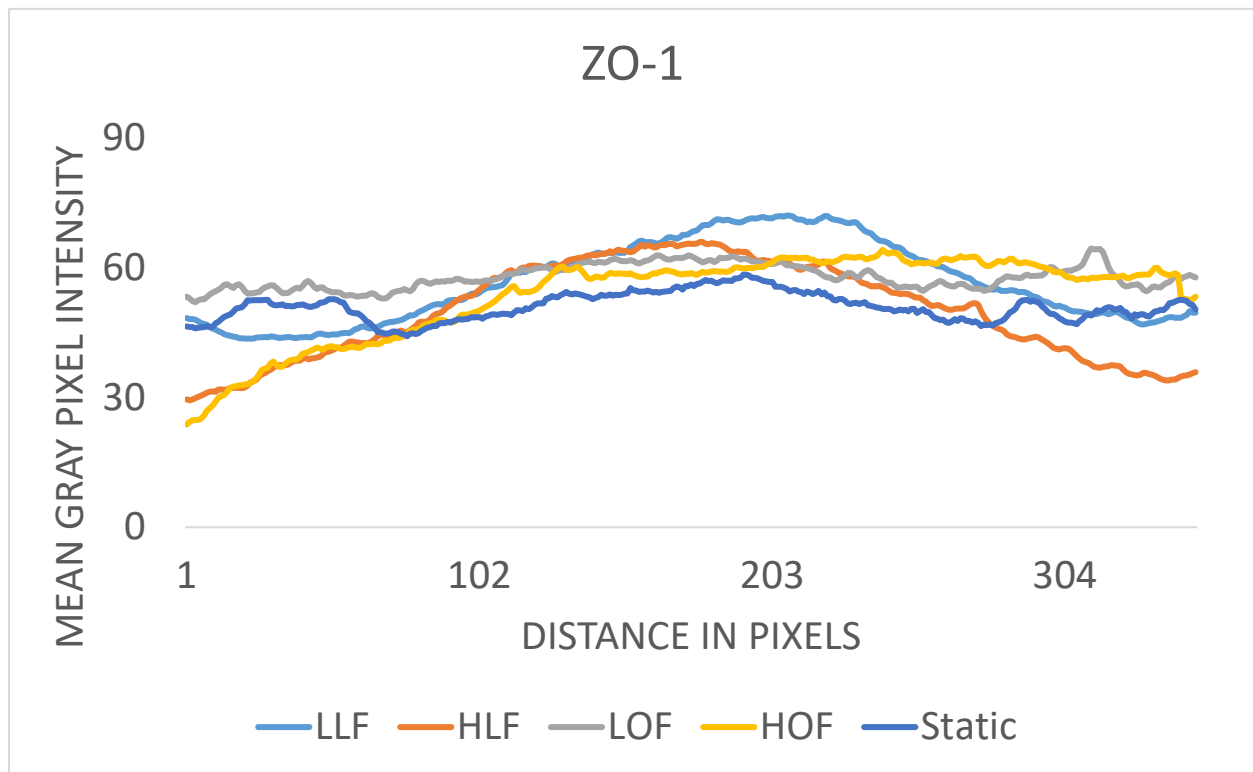
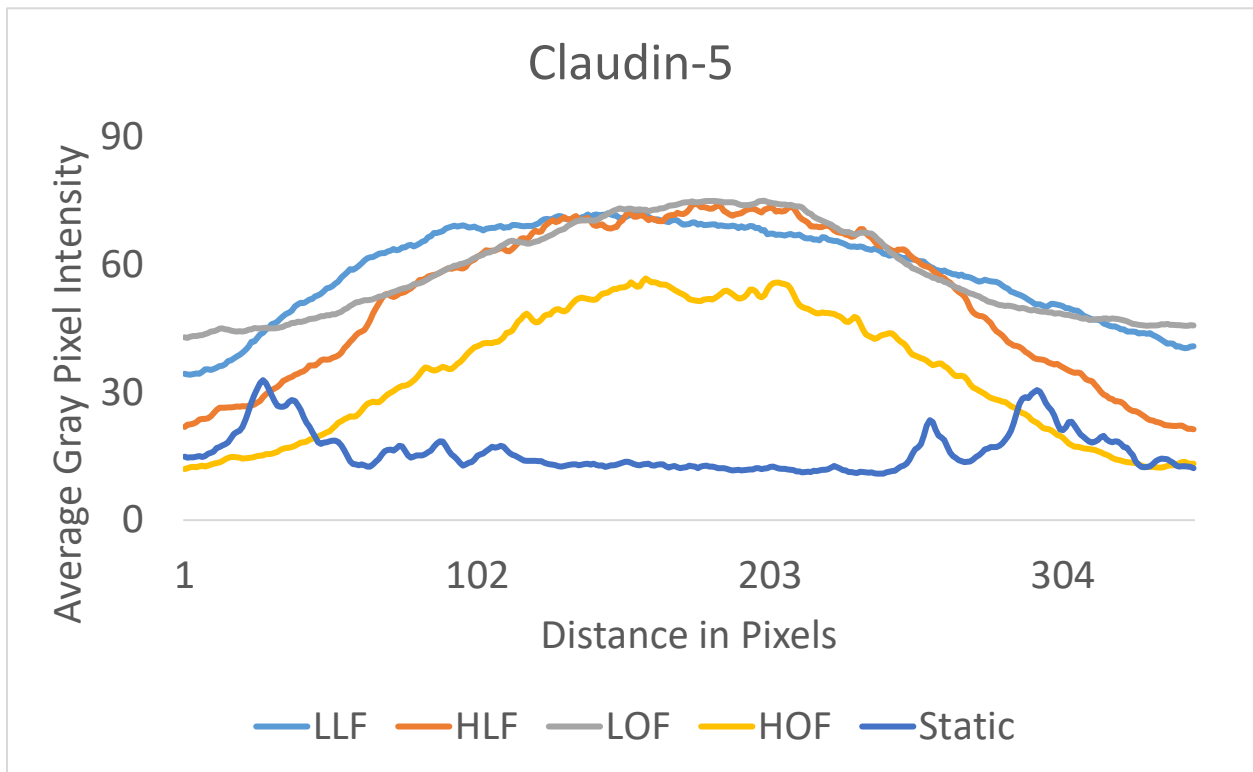


Figure 6: Graph of ZO-1 Protein Intensity

3.2 Claudin-5 Measured Length Data

The graph of Claudin-5 displays a consistent trend between all four flow regimes around the periphery of the cell. The graphed results show an increase in pixel intensity between the LLF and LOF on the LE and TE of the measurement. The graph also shows a consistent decrease in pixel intensity along LE - TE and center of the measurement between the HLF and the HOF followed by the same decrease around the periphery of the cell in these two flow regimes. The graph shows a decrease in pixel intensity around the periphery measurements between LLF and HLF and this decrease is consistent between LLF and HOF. All flow regimes show an increase in pixel intensity along the center of the measurements compared to the static. This graph depicts a spike in pixel intensity around the periphery of the cells in the static conditions then smooths when a flow is introduced. LOF depicted the highest localization of pixel intensity in the center of the measurements.

Figure 7: Graph of Claudin-5 Protein Intensity



3.3 JAM-A Measured Length Data

The images from the JAM-a stains show a difference in junctional expression around the periphery of the cell between the four different conditions. The static images show a localization of intensity around the center of the cell and clear junctional expression around the periphery of the cell. There was a decrease in overall intensity along the measurement between HLF and HOF respectively. LLF displayed a drastic increase in pixel intensity along the center of the measurement compared to the other three flow regimes. The pixel intensity of leading end of the measurement for all conditions except HOF showed subtle difference in the LE-TE. Like the TJ ZO-1, LLF depicted the highest pixel intensity localized in the center of the measurement.

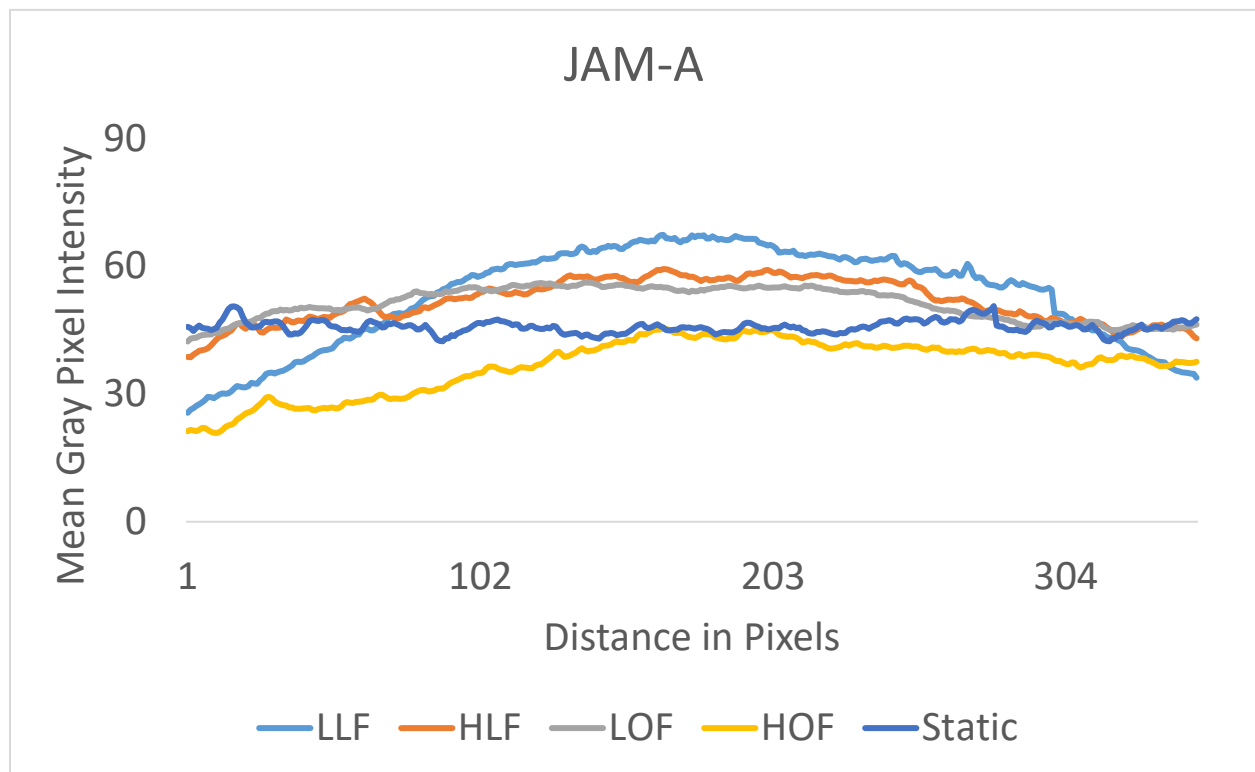


Figure 8: Graph of JAM-A Protein Intensity

3.4 VE-Cadherin

The HLF shows a significant increase in pixel intensity along the center of the measurement compared to the other 4 regimes. There is decrease in overall pixel intensity between the HLF and HOF respectively. The leading and trailing ends of the measurements displayed no significant between LLF and LOF however the LOF shows an average increase in pixel intensity along the center of the measurement compared to the LLF. Each flow regime depicts an increase in pixel intensity along the center of the measurement. There is a increase in pixel intensity from LLF to LOF along the center of the measurement.

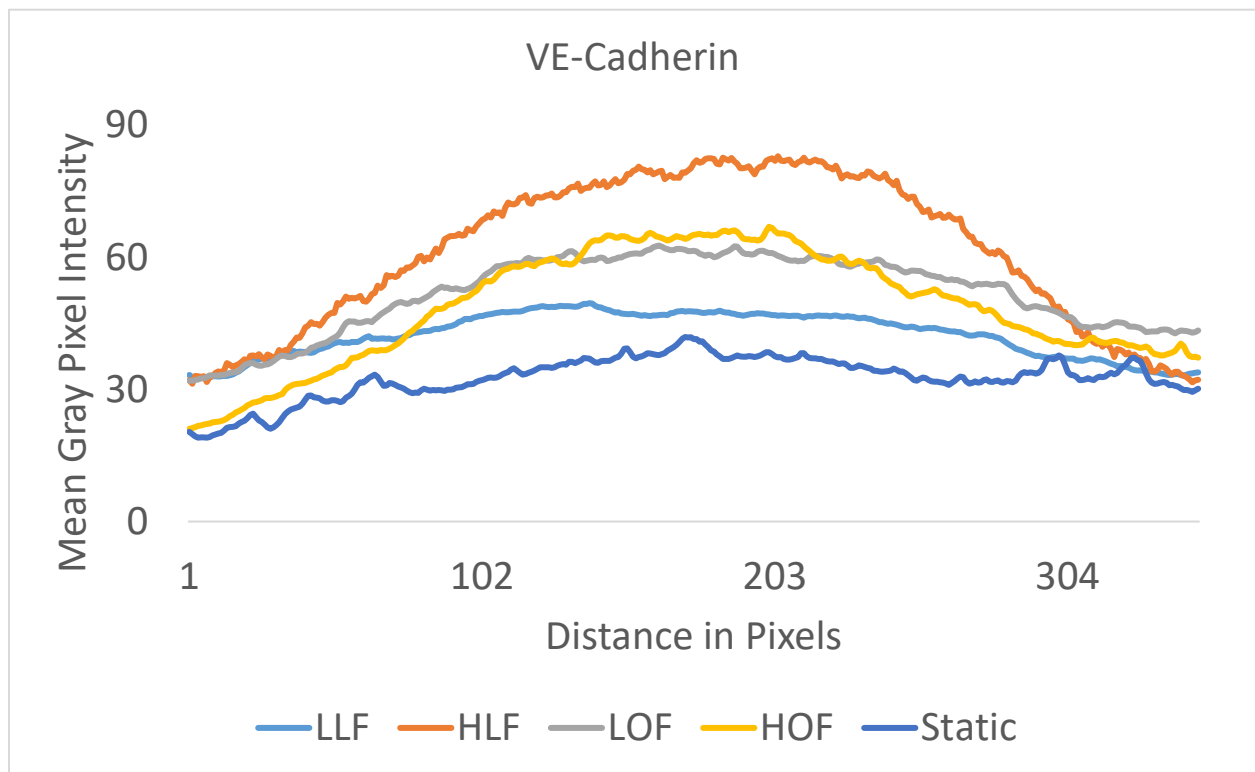


Figure 9: Graph of VE-Cadherin Protein Intensity

3.5 Results Comparison

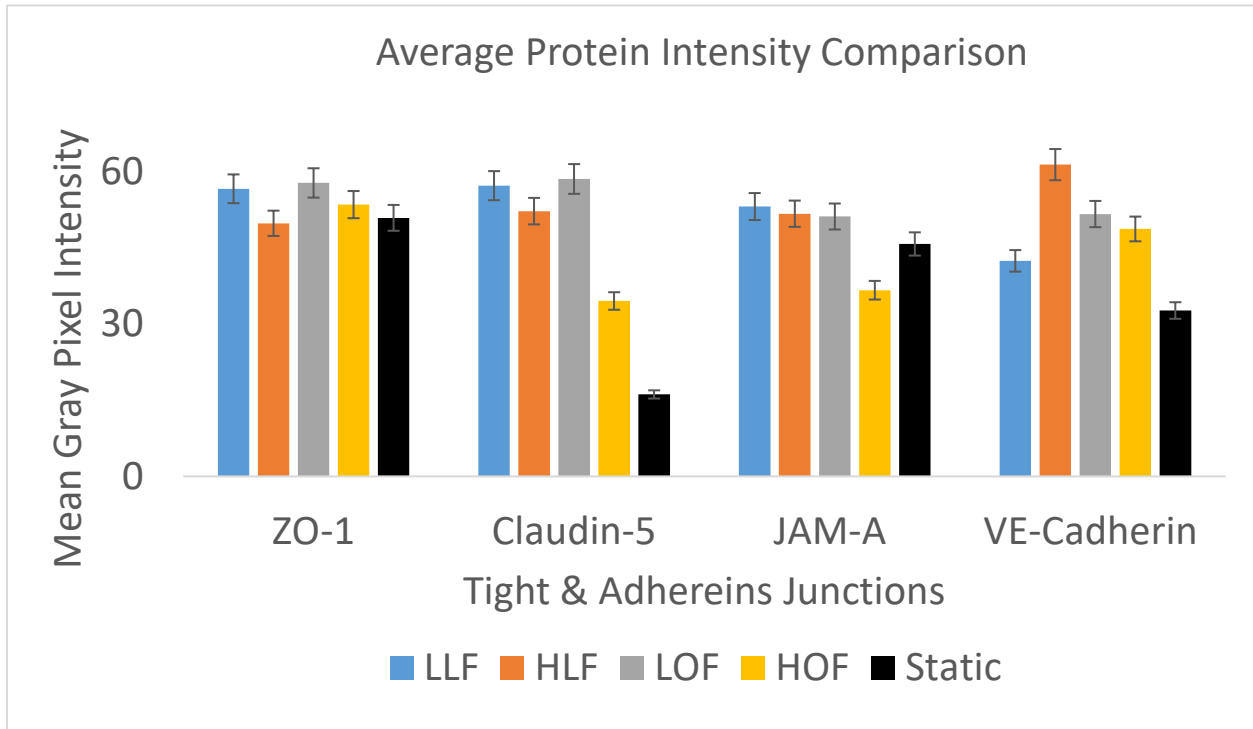


Figure 10: Average Protein Comparison Graph

The average protein comparison chart displays the average of the 350 pixel measurement length along the cell. When looking at the ZO-1 comparison we can see an overall increase in mean gray value pixel intensity of all flow regimes compared to the static. There is an increase in pixel intensity from LLF to LOF and HLF to HOF conditions. The graph also depicts a decrease in average intensity from LLF to HLF and from LOF and HOF. The graph of the Claudin-5 depicts a significant increase in pixel intensity from static to the variable flow regimes. There is a small increase in pixel intensity from LLF to LOF followed by a decrease in intensity from HLF to HOF. Like TJ ZO-1, this protein depicts a drop in intensity from LLF to HLF conditions, and a drop from LOF to HOF. JAM-A depicted a slight difference than the other TJs; there is a decrease in pixel intensity from LLF to HLF which is consistent with the previous TJs however this is a decrease in average pixel intensity from LLF to LOF. The average pixel intensity decreased from HLF to HOF and the average intensity of HLF is lower than the static condition in this protein. The AJ VE-Cadherin depicts an increase in average pixel

intensity from LLF to HLF which is an inverse relationship compared to the average intensities of the TJs. Unlike the TJs pixel intensity increases from LLF to LOF however we see a decrease in intensity from HLF to HOF which we find in the TJs. All flow induced regimes increase average pixel intensity compared to the static condition.

Table 1: Table of Average Protein Intensity Comparison

	Static	LLF	HLF	LOF	HOF
ZO-1	-	↑	↓	↑	↑
Claudin-5	-	↑	↑	↑	↑
JAM-A	-	↑	↑	↑	↓
VE-Cadherin	-	↑	↑	↑	↑

Table 2: Paired Student t-Test Results

	LLF		HLF		LOF		HOF	
	t-stat	t-critical	t-stat	t-critical	t-stat	t-critical	t-stat	t-critical
ZO-1	-13.9014	1.966824003	2.003478	1.966824003	-51.9864	1.966824003	-5.29965	1.966824003
Claudin- 5	-56.3193	1.966804223	-32.1697	1.966804223	-54.2157	1.966804223	-18.5271	1.966804223
JAM-A	-30.4801	1.966804223	-19.7959	1.966804223	-22.3058	1.966804223	24.86131	1.966804223
VE-Cadherin	-44.4457	1.966804223	-37.2098	1.966804223	-67.1228	1.966804223	-33.8155	1.966804223

Table 1 shows the general difference in the average gray value pixel intensity between each of the flow regimes. The most significant differences from the chart show that the HLF from the protien ZO-1 depicts a general decrease in intensity compared to the static conditon. Also the HOF from the JAM-A protiens depicts a general decrease compared to the static conditons. Table 2 depicts a paired t-test statistical analysis conducted with the results and the results mirror the results presnted in Table 1. This statistical analysis helps simplify the mean protient intensity difference between each flow regime compared to the respective static conditons.

CHAPTER 4 DISCUSSION

Our findings show an increase in pixel intensity from the LLF to the LOF along the boundary of the cells in both TJs ZO-1 & Claudin 5; TJs showed an overall increase in pixel intensity in all shear conditions compared to static conditions. Claudin-5 depicts a consistent difference in pixel intensity along the leading and trailing end of the measurement; AJs showed an inverse relation between LLF and HLF; in JAM-A, LLF had the highest intensity. However, VE-Cadherin had the highest average value to be from the HLF. The AJs did not show a consistent difference along the leading and trailing ends of the measurements compared to the TJs. The data in the ZO-1 set shows an increase in periphery intensity from LLF to LOF, however there this is not the case for HLF and HOF. HLF is higher than HOF in the leading end of the periphery cell. The results from the variable flow experiments depict significant differences in TJ and AJ structures between the laminar unidirectional flows and the oscillatory flows. We can see a clear upregulation of ZO-1 from Figure 1B and 1D which is also shown in Graph 1. There is a general increase in localization with pixel intensity over the nucleus under HLF conditions, even though all protein expression was downregulated during this flow regime. Surprisingly, TJ Claudin-5 shows the most localization to the nucleus after fluid flow experiments however the average mean pixels values appear to show no difference in graph 4. The most interesting differences were in the TJ ZO-1. We found that junctions were more localized around the cell from static and low laminar flow conditions to the oscillatory. As society begins to understand the role of mechanical forces on cell-cell junction response, this study aims to experimentally show various cell-cell junction responses to the different flow regimes specific to brain microvascular endothelial cells. Studies have shown that average low shear stress induce plaque buildup and add to atherosclerotic regions; in experiments that we have conducted the LLF in the TJs showed the strongest pixel intensity compared to the static condition (Dewey). Following the LLF, the LOF displayed stronger signals in fluorescent intensity; the TJ ZO-1 looked larger and displayed brighter fluorescent intensity than the static image.

Studies have shown that a decrease in TJ expression increases barrier permeability, which has been attributed to various neurodegenerative diseases such as Multiple Sclerosis (Tzung). Our findings show that TJs become more localized around the nucleus of the cell under high flow conditions and increase in intensity from low laminar to low oscillatory conditions which implies TJs localization can be flow dependent. We observed a decrease in intensity in TJs ZO-1, Claudin-5, and JAM-A under high flow conditions which implies barrier permeability may increase under larger fluid shear. Our findings suggest that bbb structure is flow-regime dependent and we therefore believe that these finds will be useful to the field of drug delivery in the bbb. We can conclude that the flow induced fluid shear stress changes cell-cell morphology organization, and potentially the junctional expression.

These results further add the claim of regions of low flow being susceptible to plaque buildup due to the increase in junctional response needed to maintain homeostasis. These results add to the claim by displaying that regions with low oscillatory showing an even stronger TJ intensity; demonstrating that atherosclerotic regions with oscillating flow regimes can induce similar or stronger outcomes then low laminar flow regimes. Our results show an overall decrease in junctional express in regions with HOF then LOF, these rules justify claims of regions that experience a High flow exhibit less plaque buildup then low flow. These results can be used to further claims that induced changes in blood flow (i.e. exercise) can reduce plaque buildup in the body's vasculature. By understanding how various flow regimes affect cell-cell junction organization under fluid shear, we can use this knowledge to target certain treatment therapies to various neurodegenerative diseases.

LIST OF REFERENCES

- A, Taddei. "Endothelial Adherens Junctions Control Tight Junctions by Ve-Cadherin-Mediated Upregulation of Claudin-5." *Nature - Cell Biology*, 2008. Vol. 10. Print.
- Bergert, Martin. "Confocal Reference Free Traction Force Microscopy." *Nature - Communications*, 2016. Vol. 7. Print.
- Cucullo. "The Role of Shear Stress in Blood-Brain Barrier Endothelial Physiology." *Journal of Biomedical Medicine BMC Neuroscience*, 2011. Vol. 12. Print.
- Davies, P.F. "Turbulent Fluid Shear Stress Induces Vascular Endothelial Cell Turnover in Vitro." *Proceedings of the National Academy of Sciences of the United States of America*, 1986. Vol. 83. Print.
- Dewey, C.F. "The Dynamic Response of Vascular Endothelial Cells to Fluid Shear Stress." *Journal of Biomechanical Engineering* 1981. Vol. 10. Print.
- Miao, Hui. "Effects of Flow Patterns on the Localization And Expression of Ve-Cadherin at Vascular Endothelial Cell Junctions: In Vivo and in Vitro Investigations " 2005. 77-89. Vol. 42. Print.
- Miura, Shigenori. "Fluid Shear Triggers Microvilli Formation Via Mechanosensitive Activation of Trpv6." *Nature - Communications*, 2015. Vol. 6. Print.
- Nardone, Giorgia. "Yap Regulates Cell Mechanics by Controlling Focal Adhesion Assembly." *Nature - Communications*, 2017. Vol. 8. Print.
- Noria, Sabrena. "Transient and Steady-State Effects of Shear Stress on Endothelial Cell Adherens Junctions." *Journal of the American Heart Association*, 1999. 504-14. Vol. 85. Print.

- OC, Colgan, and Ferguson G. "Regulation of Bovine Brain Microvascular Endothelial Tight Junction Assembly and Barrier Function by Laminar Shear Stress." 6 ed: American Physiological Society, 2007. Print.
- Sei, Yoshitaka. "Detection of Frequency-Dependent Endothelial Response to Oscillatory Shear Stress Using a Microfluidic Transcellular Monitor." *Nature - Scientific Reports*, 2017. 7 vols. Print.
- Stamatovic, M Svetlana. "Brain Endothelial Cell-Cell Junctions: How to "Open" the Blood Brainbarrier." 2008. 179-92. Vol. 6. Print.
- Tzung, Hsiai K. "Endothelial Cell Dynamics under Pulsating Flows: Significance of High Versus Low Shear Stress Slew Rates." *Analysis of Biomedical Engineering*, 2002. 646-56. Vol. 30. Print.
- Vedula, Iason. "Effect of Flow on Targeting and Penetration of Angiopep-Decorated Nanoparticles in a Microfluidic Model Blood-Brain Barrier." *PLOS*, 2018. Print.
- Womersley, J.R. "Oscillatory Flow in Arteries: The Constrained Elastic Tube as a Model of Arterial Flow and Pulse Transmission." Dayton, Ohio: Institute of Physics and Engineering in Medicine, 1957. 178. Vol. 2. Print.